RSC Advances

PAPER

View Article Online
View Journal | View Issue

Cite this: *RSC Adv.*, 2020, **10**, 1966

Rapidly detecting antibiotics with magnetic nanoparticle coated CdTe quantum dots†

Chao-Xi Chen,[a] Yu-Han Li,[a] Yun-Lu Zhou,[a] Jun-Hao Zhang,[a] Qi-Zhuang Wei,[a] Tao Dai*[b] and Lu Wang *[a]

Received 26th November 2019
Accepted 30th December 2019

DOI: 10.1039/c9ra09894a

rsc.li/rsc-advances

A reusable magnetic-quantum dot material (MNP–SiO_2–QD) with good magnetic properties and high fluorescence retention was successfully fabricated from linked magnetic nanoparticles and quantum dots. The resulting material can qualitatively and quantitatively detect four kinds of antibiotics and maintain high recovery rates.

Antibiotics are essential low molecular weight chemicals that are generally used for therapeutic and prophylactic purposes in the livestock and poultry industries.[1] Also, veterinary drugs can also promote weight growth and improve breeding efficiency. However, indiscriminate usage has led to the accumulation of drugs in animal tissues and organs, which might lead to allergic reactions and bacteria resistance.[2] Furthermore, drug residues can also be present in milk, eggs and other animal products. These drug residues can be toxic to humans and threaten their health if present above certain levels.[3–5] Therefore, drug residues are an important issue in the field of food and animal feed safety.

In order to protect human health and ensure food security, the European Union (EU) has established maximum drug residue limits in livestock.[6] Various methods are used to detect these veterinary residues, including high-performance liquid chromatography (HPLC),[7] mass spectrometry (MS)[8] and capillary electrophoresis (CE).[9] However, these methods require expensive equipment and time-consuming procedures. Solid-phase extraction (SPE) is generally used to detect medical residues,[10] however, this method is not sensitive enough. Although enzyme-linked immunosorbent assays can rapidly analyze drug residues, they cannot be used to monitor multiple residues simultaneously.[11] Thus, the development of rapid multiplex detection methods for drug residues is necessary and urgent for regulating and monitoring food safety. Recently, nanomaterials have been used as candidates for residue detection. Quantum dots (QDs) have attracted attention due to their electrical and fluorescence properties.[12–14] For example, QDs have been applied to detect drug residues *via* electrochemiluminescence because of their electrical characteristics.[15–18] Li's group[15] developed an electrochemiluminescence immunosensor based on CdSe QDs that could be a good way to analyze salbutamol residues. Zhou's group[16] demonstrated an electrochemical protocol for detecting multiple antibiotics and their residues in milk samples, employing QDs as electrochemical tags that could reflect the identities and concentrations of veterinary residues. However, these electrochemiluminescence methods require complicated synthetic procedures and electrochemical equipment. It is necessary to establish more rapid, accurate and sensitive assay methodologies. To this end, the fluorescence properties of QD create the opportunity for drug residue detection.[19–25] Walia and Acharya[25] synthesized CdS QDs coated with glutathione for the selective detection of dicofol. Dicofol can interact with –COOH and $–NH_2$ in glutathione. The interaction between dicofol and glutathione can increase the fluorescence intensity. Furthermore, Li's group[26] fabricated a core–shell complex with CdTe QDs and silicon spheres that was used as a fluorescence probe for detecting pesticides. Fluorescence detection has the advantages of high sensitivity, being simple and rapid, and needing no special testing equipment. However, this method is limited by its recycling properties. Therefore, an important development direction is achieving reusable quantum dots in the field of antibiotic detection. Magnetic nanoparticles have drawn interest due to their high magnetic responsiveness, easy separation and low toxicity, and they could be the best choice for achieving reusability. In the reported literature, magnetic materials have weak fluorescence intensities,[27] and studies involving the detection of drug residues using quantum dot fluorescence properties are rare.[28–30]

Therefore, considering the perfect fluorescence properties of quantum dots and the magnetic properties of Fe_3O_4, we have successfully fabricated a magnetic-quantum dot material (MNP–SiO_2–QD) with high fluorescence retention and reusability based on the properties of typical CdTe QDs and magnetic nanoparticles (MNPs). In this work, the fluorescence intensity of MNP–SiO_2–QD could reach 1300, which is

[a]College of Life Science & Technology, Southwest Minzu University, Chengdu 61004, China. E-mail: luwangbest@163.com; chaoxi8832@163.com

[b]College of Chemistry & Environmental Protection Engineering, Southwest Minzu University, 610041, China. E-mail: tdaicat@163.com

† Electronic supplementary information (ESI) available. See DOI: 10.1039/c9ra09894a

significantly higher than other reported magnetic materials,[27] and the fluorescence retention rate could reach 60%. At the same time, MNP–SiO_2–QD can be reused because of its magnetic responsiveness. After five cycles of use, the fluorescence intensity of MNP–SiO_2–QD could still retain 50% of its initial level. In addition, the material can qualitatively and quantitatively detect antibiotics within 5 minutes, and detection had no dependence on the substrate used. Therefore, MNP–SiO_2–QD showed good prospects in the field of veterinary drug residue detection, providing a template for the development of new antibiotic detection methods, and ensuring the development of food safety.

We constructed a kind of quantum dot material coated with magnetic nanoparticles, possessing excellent fluorescence properties and magnetic responsiveness, which could be used to detect antibiotics within 5 minutes. This material not only showed an improvement in the fluorescence intensity compared to other magnetically coated quantum dots, but it also achieved good recycling performance, showing potential for use in the field of rapid veterinary drug residue detection.

Results and discussion

The fabrication of MNP–SiO_2–QD nanoparticles is illustrated in Fig. S1.† CdTe QDs with high fluorescence intensity were prepared *via* a conventional hydrothermal method, and magnetic nanoparticles (MNP–SiO_2) with a porous structure were constructed *via* a co-precipitation method. Finally, MNP–SiO_2–QD with magnetic responsiveness, recyclability and a high fluorescence retention rate was obtained *via* a sol–gel method.

To demonstrate the successful synthesis of MNP–SiO_2, it was studied using FT-IR spectroscopy. The IR spectra of MNPs and MNP–SiO_2 in the range of 500 to 4000 cm^{-1} are shown in Fig. 1a. For the MNPs, the two strong absorption bands at around 570 and 3438 cm^{-1} correspond to Fe–O bonds and –OH stretching vibrations from Fe_3O_4. Small shifts can be observed in these two characteristic bands after coating with SiO_2. Upon comparing MNP–SiO_2 and MNP–SiO_2–QD with the MNPs, Si–O–Si absorption was observed at 1084 cm^{-1}. These results indicated that SiO_2 was successfully coated on the surface of the MNPs. Furthermore, by comparing the fluorescence properties of the MNPs, MNP–SiO_2, and MNP–SiO_2–QD, the MNP–SiO_2–QD material had perfect fluorescence properties, while the MNP and MNP–SiO_2 materials did not have fluorescence properties under a UV lamp (Fig. 1d). Meanwhile, we analyzed the Fe, Si, O, Cd, and Te elements in the material, as shown in Fig. 3. According to the above results, the MNP–SiO_2–QD material was successfully prepared. Comparing the fluorescence intensities of the QDs and MNP–SiO_2–QD, the fluorescence retention rate was maintained at 40% (Fig. S2†). Therefore, it can be proved that MNP–SiO_2–QD with good fluorescence properties was successful fabricated.

For further investigating the crystal structures of the MNPs, MNP–SiO_2 and MNP–SiO_2–QD, the XRD diffraction patterns are shown in Fig. 1b. All the diffraction peaks of MNP–SiO_2 and MNP–SiO_2–QD were consistent with those of the MNPs ((2 2 0), (3 1 1), (4 0 0), (4 2 2), (5 1 1), and (4 4 0) indices), which

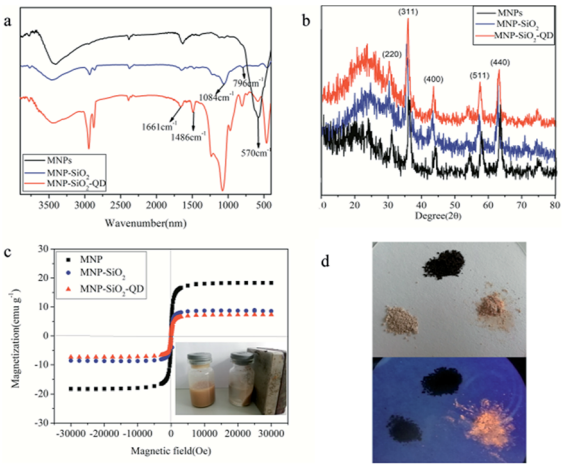

Fig. 1 (a) The FTIR spectra of the MNPs, MNP–SiO_2 and MNP–SiO_2–QD. (b) The XRD patterns of the MNPs, MNP–SiO_2 and MNP–SiO_2–QD. (c) The magnetization curves of the MNPs, MNP–SiO_2 and MNP–SiO_2–QD. (d) Images of the MNPs (top), MNP–SiO_2 (bottom left) and MNP–SiO_2–QD (bottom right) without (upper panel) and with (lower panel) UV lamp irradiation.

indicated that the modification of the MNPs with SiO_2 and QDs did not change the crystal form of Fe_3O_4. The vibrating-sample magnetometer (VSM) technique was used to measure the magnetization properties and magnetization values at room temperature. The hysteresis loops from the MNPs, MNP–SiO_2 and MNP–SiO_2–QD are shown in Fig. 1c. According to the results, the coercivity and remanence values of all samples were zero, which suggested that the MNPs, MNP–SiO_2 and MNP–SiO_2–QD were superparamagnetic. The saturation magnetization values for MNP–SiO_2–QD and the MNPs were 7.12 and 18.08 emu g^{-1}, respectively. Although the saturation magnetization value of MNP–SiO_2–QD was a little lower than that of the MNPs, due to the presence of nonmagnetic inorganic particles, it was large enough that the particles could be separated from solution under an external magnetic field.

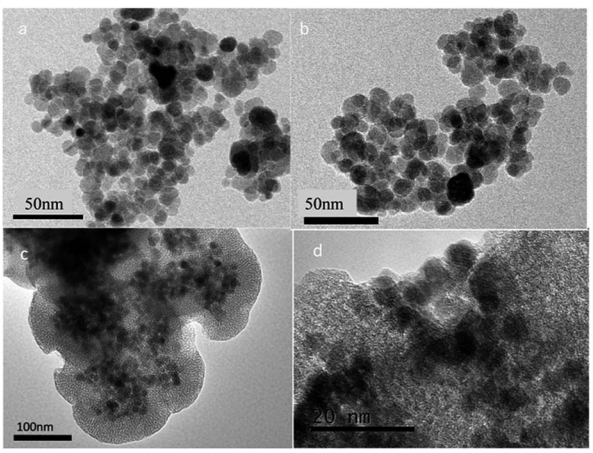

Fig. 2 TEM images of (a) the MNPs, (b) MNP–SiO_2, and (c and d) MNP–SiO_2–QD.

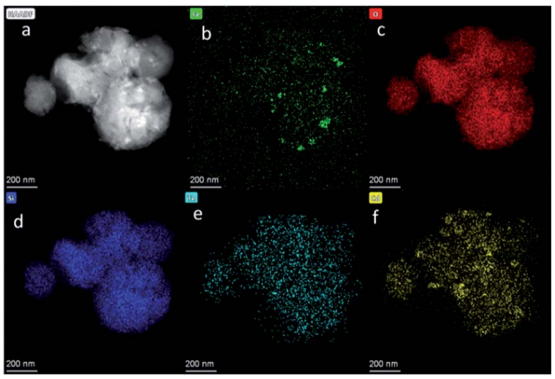

Fig. 3 TEM mapping of MNP–SiO_2–QD: (a) a TEM image of MNP–SiO_2–QD; (b) Fe element mapping; (c) O element mapping; (d) Si element mapping; (e) Te element mapping; and (f) Cd element mapping.

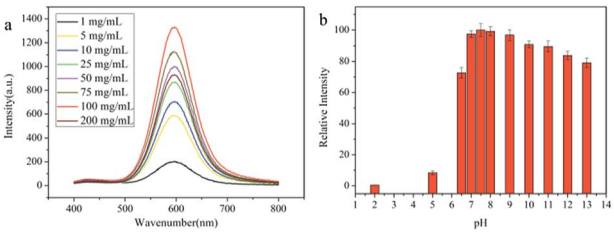

Fig. 4 (a) The fluorescence spectra of MNP–SiO_2–QD at different concentrations. (b) The relative fluorescence intensities of MNP–SiO_2–QD at different pH values. The fluorescence intensity of MNP–SiO_2–QD at a pH value of 7.5 was set as 100%.

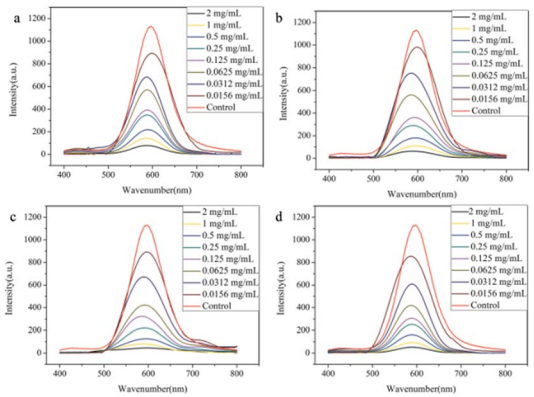

Fig. 5 The fluorescence spectra of MNP–SiO_2–QD in the presence of different concentrations of different antibiotics: (a) enrofloxacin, (b) ceftiofur, (c) doxycycline, and (d) chloramphenicol.

TEM images of the QDs (Fig. S3†), the MNPs, MNP–SiO_2, and MNP–SiO_2–QD are given in Fig. 2. All the particles were spherical. The DLS results show the narrow size distribution of the MNPs, MNP–SiO_2 and MNP–SiO_2–QD (Fig. S8†). The average size of MNP–SiO_2–QD was much bigger than those of the MNPs and MNP–SiO_2, which indicated that TEOS formed a coating layer on the surfaces of the MNPs. According to the element

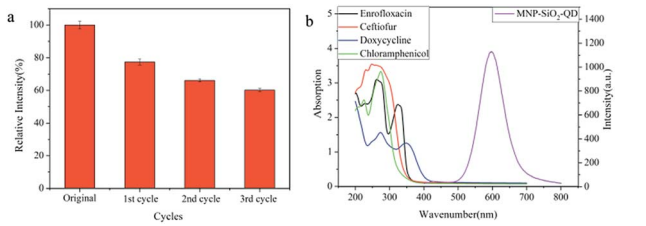

Fig. 6 (a) The relative fluorescence intensities of pristine MNP–SiO_2–QD and reused samples. (b) The UV-vis absorption spectra of the antibiotics and the fluorescence spectrum of MNP–SiO_2–QD.

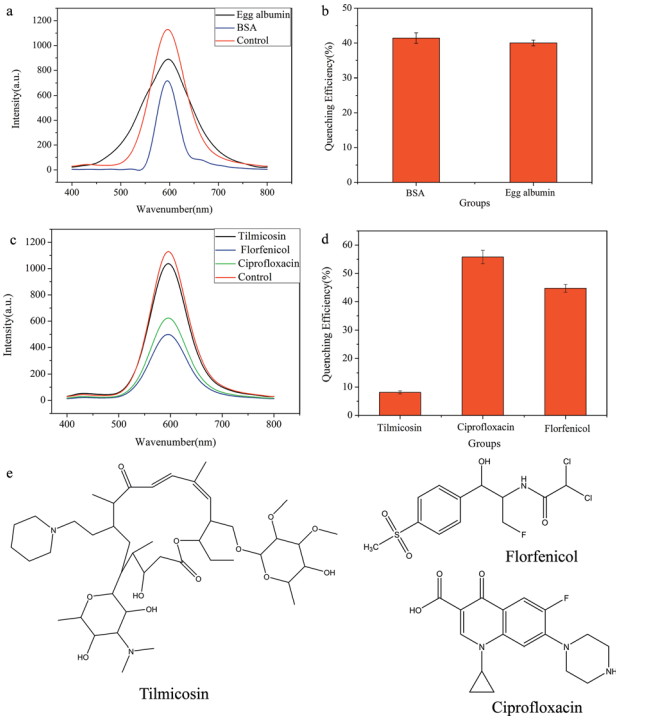

Fig. 7 The fluorescence spectra (a) and quenching efficiencies (b) of MNP–SiO_2–QD with doxycycline in different solutions. The fluorescence spectra (c) and quenching efficiencies (d) with different antibiotics. (e) The structures of the different antibiotics.

mapping results, the MNP–SiO_2–QD material contained Fe, Si, O, Cd, and Te (Fig. 3). The above results indicate that the MNP–SiO_2–QD material was successfully prepared.

In order to determine the fluorescence properties of MNP–SiO_2–QD, we studied the differences in the fluorescence intensities of the materials under different pH conditions (Fig. 4b). The strongest fluorescence was at a pH value of 7.5, which was set as 100%. According to the results, the fluorescence intensity of MNP–SiO_2–QD significantly decreased under acidic conditions. However, the fluorescence intensity can remain at more than 80% under alkaline conditions. Therefore, we chose to carry out subsequent tests in neutral or weak alkaline aqueous solutions. In addition, to select the optimal detection concentration, we also compared the fluorescence intensities at different concentrations. The results are showed in Fig. 4a. No

Table 1 The concentration and recovery rate of doxycycline in BSA and egg albumin solutions

Substrate	Standard concentration (mg mL^{-1})	Obtained concentration (mg mL^{-1})	Recovery rate
BSA	0.0200	0.0193	96.5%
Egg albumin	0.0200	0.0161	80.5%

decrease in fluorescence intensity occurred as the concentration of MNP–SiO_2–QD was increased to 100 mg mL^{-1}, indicating the excellent dispersibility and stability, laying the foundation for the strong fluorescence properties of MNP–SiO_2–QD. The fluorescence intensity remained at 40% of that of a CdTe quantum dot solution (in Fig. S2†). When the concentration was increased to 200 mg mL^{-1}, the fluorescence intensity sharply decreased. The main reason for this was that as the concentration increased, the material aggregated. Therefore, the fluorescence intensity decreased. As a result, we chose a concentration of 100 mg mL^{-1} for use in further tests.

Antibiotics play an important role in the treatment of animal diseases, but their use may cause residues in animal products. To ensure food safety, rapid and efficient detection methods for antibiotics need to be established. We used MNP–SiO_2–QD for the detection of multiple antibiotics and evaluated the reusability of the material. In Fig. 5, enrofloxacin, ceftiofur, doxycycline and chloramphenicol are shown to quench the fluorescence intensity of MNP–SiO_2–QD. Also, with an increase in the concentration, the fluorescence quenching effect of the material was better. It was indicated that MNP–SiO_2–QD could qualitatively detect the four kinds of antibiotics. To evaluate the quantitative detection performance towards antibiotics, a linear relationship was established between the antibiotic concentration and I_0/I (I_0 and I are the median fluorescence intensities of MNP–SiO_2–QD in the absence and presence of an antibiotic). The results showed that I_0/I had a good linear relationship with concentration for the four antibiotics (Fig. S4†). Thus, MNP–SiO_2–QD can qualitatively and quantitatively detect the four antibiotics. MNP–SiO_2–QD could detect antibiotics through the quenching of the fluorescence of the quantum dots. The detected antibiotics could quench the fluorescence of the quantum dot in two ways: fluorescence resonance energy transfer (FRET); and electron transfer.[31,32] The FRET fluorescence quenching mechanism is mainly based on an overlapping region between the ultraviolet absorption spectrum of the substrate being detected and the fluorescence spectrum of the quantum dots. Thus, excitation of the quantum dots was accompanied by a FRET process. The electron transfer mechanism needs organic substrates to act as electron acceptors or electron donors to quench the luminescence. The fluorescence spectrum of MNP–SiO_2–QD and the UV-vis spectra of the antibiotics are shown in Fig. 6b. There are no overlapping regions between the fluorescence and UV-vis spectra. At the same time, the diameters of MNP–SiO_2–QD before and after antibiotic addition were nearly the same (Fig. S7†). The antibiotics did not cause the aggregation of the particles. Thus, it was indicated that electron transfer was the main cause of the fluorescence quenching.

The used MNP–SiO_2–QD material could be recycled and reused after simple treatment. Under an external magnetic field, the material can be quickly separated from solution, and MNP–SiO_2–QD was washed repeatedly with alcohol solution. After drying, MNP–SiO_2–QD can be used for another cycle. From fluorescence spectra measurements, the fluorescence intensity of the first cycle post-recovery was 80% of the initial fluorescence intensity. After three recycling cycles, the fluorescence intensity could still be maintained at 60% (Fig. 6a). At the same time, the magnetic properties of the material did not change significantly (Fig. S5†). These results are sufficient to show that MNP–SiO_2–QD had good reusability.

To further explore the universal antibiotic detection performance, we measured the fluorescence quenching efficiency after mixing a known concentration of doxycycline (0.02 mg mL^{-1}) with egg albumin and bovine serum albumin (BSA) (Fig. 7a and b). The actual antibiotic content was calculated based on the above-obtained standard curve. As shown in Table 1, the antibiotic concentration was measured to be 0.01934 mg mL^{-1} in BSA solution, and the recovery rate reached 96.59%. The obtained antibiotic concentration and recovery rate in the egg albumin solution were slightly lower than in BSA solution. Therefore, MNP–SiO_2–QD had good detection efficiency for antibiotics in different substrate solutions.

We wondered whether MNP–SiO_2–QD could detect other antibiotics with conjugated structures. We selected three antibiotics as model molecules, tilmicosin, florfenicol and ciprofloxacin, which are commonly used in animal therapy. The results are shown in Fig. 7c and d. These three antibiotics have different degrees of quenching effects on MNP–SiO_2–QD, and it could also be used as a platform for detecting these antibiotics through establishing standard curves for these antibiotics. Therefore, the MNP–SiO_2–QD material we constructed showed good detection performance toward various antibiotics.

Conclusions

In summary, we have constructed a material with fluorescence and magnetic properties to detect antibiotics within 5 minutes. MNP–SiO_2–QD could not only qualitatively analyze, but also quantitatively detect, the presence of antibiotics (such as fluoroquinolones, tetracyclines, chloramphenicol, and cephalosporins). At the same time, MNP–SiO_2–QD demonstrated good recycling performance and high recovery rates in different solutions. After 5 cycles of use, the fluorescence was maintained at 50% of the initial level. Thus, MNP–SiO_2–QD was expected to

be a good candidate as a detection method in food safety and testing areas.

Conflicts of interest

There are no conflicts to declare.

Acknowledgements

This work was funded by the National Natural Science Foundation of China (Grant No. 21908183 and 51573187), and Fundamental Research Funds for Central Universities, Southwest Minzu University (Grant No. 2019NQN49).

Notes and references

1 G. Bretschneider, J. C. Elizalde and F. A. Pérez, *Livest. Sci.*, 2008, **114**, 135–149.
2 M. Reig and F. Toldrá, *Meat Sci.*, 2008, **78**, 60–67.
3 R. P. Lopes, R. C. Reyes, R. Romero-González, A. G. Frenichand and J. L. M. Vidal, *Talanta*, 2012, **89**, 201–208.
4 R. E. Baynes, K. Dedonder, L. Kissell, D. Mzyk, T. Marmulak, G. Smith, L. Tell, R. Gehring, J. Davis and J. E. Riviere, *Food Chem. Toxicol.*, 2016, **88**, 112–122.
5 N. Liu, Z. Gao, H. Ma, P. Su, X. Ma, X. Li and G. Ou, *Biosens. Bioelectron.*, 2013, **41**, 710–716.
6 J. F. Prescott, *Anim. Health Res. Rev.*, 2008, **9**, 127–133.
7 A. Masiá, M. M. Suarez-Varela, A. Llopis-Gonzalez and Y. Picó, *Anal. Chim. Acta*, 2016, **936**, 40–61.
8 W. Jia, X. Chu, Y. Ling, J. Huang and J. Chang, *J. Chromatogr. A*, 2014, **1347**, 122–128.
9 R. Aebersold and M. Mann, *Nature*, 2003, **422**, 198.
10 A. Boscher, C. Guignard, T. Pellet, L. Hoffmann and T. Bohn, *J. Chromatogr. A*, 2010, **1217**, 6394–6404.
11 M. Meng and R. Xi, *Anal. Lett.*, 2011, **44**, 2543–2558.
12 I. U. Arachchige and S. L. Brock, *J. Am. Chem. Soc.*, 2007, **129**, 1840–1841.
13 I. L. Medintz, H. T. Uyeda, E. R. Goldman and H. Mattoussi, *Nat. Mater.*, 2005, **4**, 435.
14 X. Xie, D. Ma and L.-M. Zhang, *RSC Adv.*, 2015, **5**, 58746–58754.
15 J. Zhang, F. Cai, A. Deng and J. Li, *Electroanalysis*, 2014, **26**, 873–881.
16 J. Xue, J. Liu, C. Wang, Y. Tian and N. Zhou, *Anal. Methods*, 2016, **8**, 1981–1988.
17 D. Tang, L. Hou, R. Niessner, M. Xu, Z. Gao and D. Knopp, *Biosens. Bioelectron.*, 2013, **46**, 37–43.
18 J. Shan, R. Li, K. Yan, Y. Zhu and J. Zhang, *Sens. Actuators, B*, 2016, **237**, 75–80.
19 J. Wu, F. Xu, K. Zhu, Z. Wang, Y. Wang, K. Zhao, X. Li, H. Jiang and S. Ding, *Anal. Lett.*, 2013, **46**, 275–285.
20 T. Le, L. Zhu and H. Yu, *Food Chem.*, 2016, **199**, 70–74.
21 E. Song, M. Yu, Y. Wang, W. Hu, D. Cheng, M. T. Swihart and Y. Song, *Biosens. Bioelectron.*, 2015, **72**, 320–325.
22 C. Wu, N. Gan, C. Ou, H. Tang, Y. Zhou and J. Cao, *RSC Adv.*, 2017, **7**, 8381–8387.
23 Y. He, B. Zhang and Z. Fan, *Microchim. Acta*, 2018, **185**, 163.
24 X. Yu, K. Wen, Z. Wang, X. Zhang, C. Li, S. Zhang and J. Shen, *Anal. Chem.*, 2016, **88**, 3512–3520.
25 S. Walia and A. Acharya, *J. Nanopart. Res.*, 2014, **16**, 2778.
26 H. Li and F. Qu, *Chem. Mater.*, 2007, **19**, 4148–4154.
27 M. Watanabe, K. Gonda, N. Ohuchi and T. Jin, *Biomaterials*, 2012, **33**, 8486–8494.
28 Y. Zhang, S. Ge, S. Wang, M. Yan, J. Yu, X. Song and W. Liu, *Analyst*, 2012, **137**, 2176–2182.
29 J. Ruan, K. Wang, H. Song, X. Xu, J. Ji and D. Cui, *Nanoscale Res. Lett.*, 2011, **6**, 299.
30 S. Giri, D. Li and W. C. W. Chan, *Chem. Commun.*, 2011, **47**, 4195–4197.
31 L. Jia, J.-P. Xu, D. Li, S.-P. Pang, Y. Fang, Z.-G. Song and J. Ji, *Chem. Commun.*, 2010, **46**, 7166–7168.
32 R. Freeman, T. Finder, L. Bahshi and I. Willner, *Nano Lett.*, 2009, **9**, 2073–2076.

